Proc. Natl. Acad. Sci. USA
Vol. 87, pp. 6433–6435, August 1990
Biophysics

Simulation of shape changes and adhesion phenomena in an elastic model of erythrocytes

(membranes/vesicles/thermal fluctuations/unbinding/curvature energy)

S. LEIBLER* AND A. C. MAGGS†

*Service de Physique Théorique de Saclay, Laboratoire de l'Institut de Recherche Fondamentale du Commissariat a l'Energie Atomique, F-91191 Gif-sur-Yvette Cedex, France; and †Laboratoire de Physico-Chimie Théorique, Ecole Supérieure de Physique et de Chimie Industrielles, 10 rue Vauquelin, F-75231 Paris Cedex 05, France

Communicated by Michael E. Fisher, May 2, 1990 (received for review March 8, 1990)

ABSTRACT **We present simulations of a model of a closed membrane that shares important features with erythrocytes: resistance to bending and shear, membrane asymmetry, and an osmotic pressure difference between the interior and exterior. By varying a few parameters we obtain several realistic (e.g., biconcave and cup-like) shapes whose fluctuations, analogous to flickering of erythrocytes, and mutual transformations are studied in thermal equilibrium. Our simulations form a basis for quantitative analysis of recent experiments done on erythrocytes and artificial bilayer vesicles. They also predict effects that could be observed in experiments such as an "unbinding" phenomenon, i.e., a separation of adhering cells induced by thermal fluctuations.**

Mammalian erythrocytes are among the simplest systems for the study of shape changes of eukaryotic cells (1); they do not include transcellular cytoskeletons and their shape is mainly determined by elastic properties of the plasma membrane. Simple mechanical models that explained biconcave or cup-like erythrocyte shapes have been formulated (2) and studied intensively (1, 3–6). However, it is only now that one can hope to test these models quantitatively thanks to recent progress in three fields. (*i*) The molecular structure of the erythrocyte membrane and the associated protein skeleton has been elucidated (1, 7), making possible a microscopic interpretation of phenomenological parameters of the models. (*ii*) Progress has been made in experimental techniques for studying erythrocytes and bilayer vesicles (8–12). (*iii*) Through recent developments in statistical mechanics, one better understands the thermodynamic behavior of fluctuating surfaces (13).

From a statistical mechanical point of view, membranes are unique since their behavior is often governed not by surface tension but by curvature energy. For closed fluid membranes, the curvature energy (E_c) can be written as (2, 13, 14):

$$E_c[S] = \int dA \, \frac{\kappa}{2} (H - H_0)^2, \qquad [1]$$

where the integration is over the area A, H is the geometrical mean curvature, and S is the shape. Two phenomenological elastic constants enter this formula: the bending stiffness κ, typically of order of 10 k_BT, and the "spontaneous" curvature H_0, characterizing the membrane asymmetry in erythrocytes due to the presence of the associated skeleton and the differences in composition of the membrane layers (1, 7). In Eq. 1 we have neglected the compressibility term as well as the contribution $\int dA\, K$, where K is the Gaussian curvature.

The publication costs of this article were defrayed in part by page charge payment. This article must therefore be hereby marked "*advertisement*" in accordance with 18 U.S.C. §1734 solely to indicate this fact.

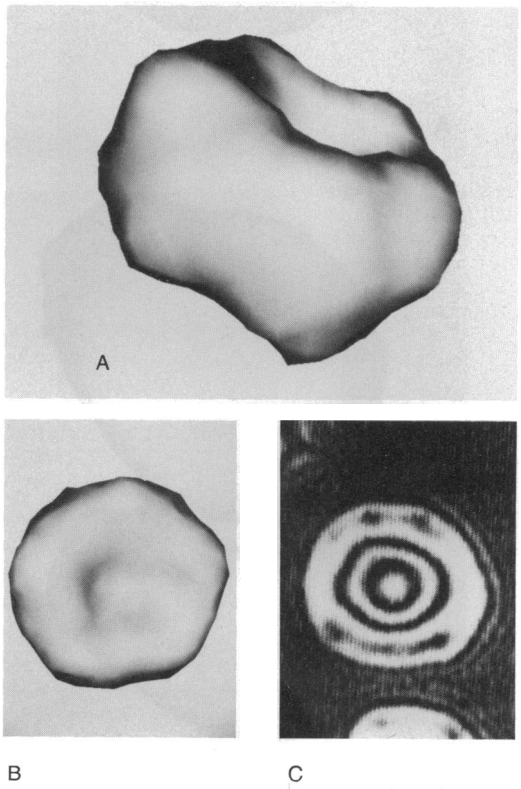

FIG. 1. (*A*) Thermally equilibrated discocyte. The surface is defined by the positions of the center of hard spheres that form 980 elementary triangles. The images are rendered using Gouraud shading. The simulation is done in the constant volume ensemble with $\kappa \approx 5.2 k_BT$; $V/V_A \approx 0.74$; and $H_0R_A \approx -1.16$, where $R_A = (A/4\pi)^{1/2}$, $V_A = (4\pi/3)R_A^3$. H_0 has a sign opposite to that of a sphere. (*B*) Top view of the same membrane. Notice that this almost circular shape still keeps a memory of the connectivity of the triangulated lattice (a regular icosahedron). (*C*) Although real skeleton nets have many more elementary spectrin triangles (22), similar effects (due to the finite density of connectivity defects) are in fact observed in erythrocytes as shown by this interferometric picture [reproduced with permission from ref. 20 (copyright E. Sackmann)].

Indeed, if the topology of the membrane does not change (e.g., a closed vesicle), this last term remains constant (13).

The problem of finding the stable shape S reduces to minimization of $E_c[S]$ with the constraints of constant A and enclosed volume V. Although this difficult problem has been solved only under simplifying conditions, shapes very similar to real discocytes and stomatocytes have been found (2, 4–6). Experiment provides an even bigger challenge: One has to take into account thermal fluctuations (15) and thus solve a thermodynamical problem rather than a mechanical one (16, 17). Recent progress in statistical mechanics of fluctuating

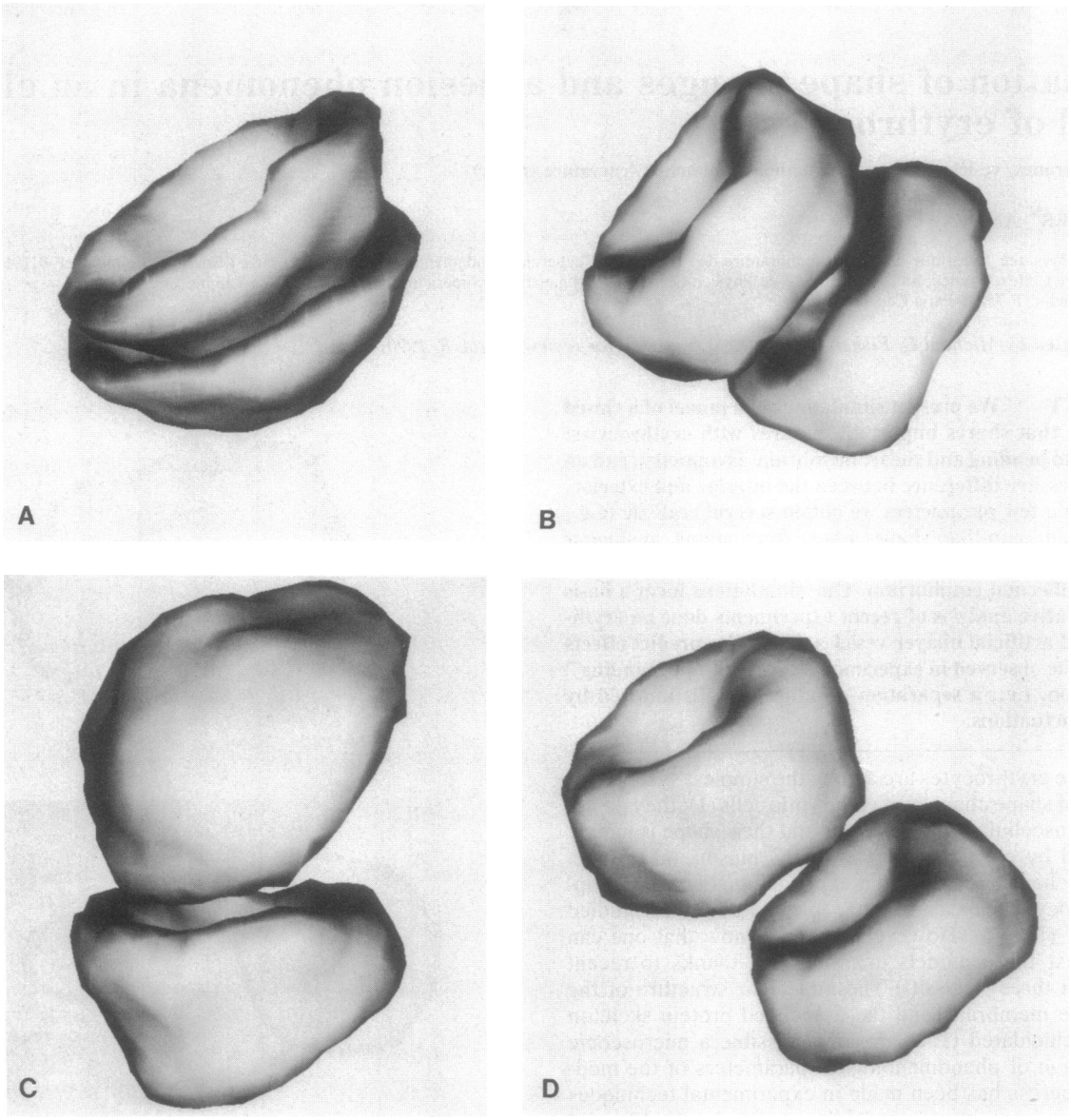

FIG. 2. Simulation of two interacting discocytes. Here we have used a pressure ensemble with $pV_A \approx 49\kappa$ and values of κ and H_0 as in Fig. 1. By decreasing the strength of the potential h, one first changes the shape of the cells [$h/\kappa = 0.28$ (*A*) or $h/\kappa = 0.056$ (*B*): The cells are adhering to each other; their separation is smaller than l]. Then thermal fluctuations provoke unbinding [$h/\kappa = 0.052$ (*C*)] and separation $h/\kappa = 0.028$ (*D*)]. Note also that for the values of h near the critical one, h_{cr}, where the unbinding occurs (*C*), the shape fluctuations of the cells are large. An unbinding transition has recently been observed for a stack of fluid lipid membranes (25). [Note that in our simulations the membranes are of finite size; thus the probability of unbinding for $h > h_{cr}$ is strictly speaking nonzero, although it is exponentially small in the number of elementary triangles and h.]

surfaces has shown that the thermodynamics of fluid membranes is very different from that of membranes with a resistance to shear (13). Erythrocyte envelopes with a skeleton containing actins and spectrins are obviously of the latter class (1). To describe these effects within a continuous elastic model, one has to add to the curvature energy $E_c[S]$ a two-dimensional elastic term (13):

$$E[S] = E_c[S] + E_{el}[S]. \quad [2]$$

Theoretical studies in which one includes a shear modulus and compressibility have produced surprising results; a free elastic membrane is no longer described by classical laws of elasticity (18, 19). Although the case of closed membranes (with a nonzero osmotic pressure difference, p) has not been studied quantitatively yet, it is possible that one has to reconsider the (classical) interpretation of measurements of elastic properties of erythrocytes, made, e.g., by video microscopy (9), micropipette techniques (8), and light interferometry (20). This is particularly difficult since the usual approximations of a planar membrane (15) or a quasispherical vesicle (10–12) are inadequate.

This motivated our study of a discretized version of the model 2 with the aid of computer simulation. The membrane is formed by a net of hard spheres of radius a and tethers (21) whose size is b. The actual values $a = 1$ and $b = 1.6$ are chosen so as to enforce self-avoidance of the membrane (21). Since the connectivity of real spectrin networks (22) remains an open question (1) (it can adjust on large time scales), we have chosen a triangulated icosahedron, leaving for future studies the role of different connectivities. Note that for a closed membrane with the topology of a sphere a coordination number of every particle cannot be equal to six and one has to introduce at least 12 defects with a coordination number of five. The spheres connected by tethers cannot move freely within the surface: the local neighborhood is

fixed as well as the maximum distance between neighbors, the elastic terms E_{el} are thus generated through entropic effects. Our discretized membrane is, therefore, a model for the bilayer–cytoskeleton envelope that presents a finite compressibility and shear modulus. To study the membrane in thermal equilibrium, the Metropolis algorithm (23) was used with a discretized version of the energy from Eq. 1. We chose a simple discretization: $E_c = \Sigma_{\langle ij \rangle} \kappa_1 \cos\theta_{ij} + \kappa_2 \sin\theta_{ij}$, where θ_{ij} is the angle between two adjacent triangles i and j. The elastic constants κ and H_0 appearing in Eq. 1 are connected through simple geometric arguments to the constants κ_1 and κ_2. Simulations were performed in a constant volume ensemble or with the addition of a compressing term pV, a constant pressure ensemble, respectively, for impermeable and permeable cells.

Fig. 1 shows a snapshot of an equilibrated membrane with κ and H_0 within a range of values for which the shape resembles a biconcave discocyte. This particular shape was obtained starting from the initial icosahedron and is thermodynamically stable. During the simulation, we monitor the time dependence of the pressure p, the radius of gyration R_G, and the energy E_c. This allows us to estimate equilibration times: a typical number of Monte Carlo steps needed to equilibrate and measure the properties of the membrane is 5×10^7, corresponding to 1.5 hr of central processing unit time on a Cray-XMP computer. To avoid metastable shapes, initial configurations were also varied: e.g., in a constant pressure ensemble, a discocyte shape can be often metastable and "decay" into a stomatocyte form. We have also observed other forms, some of them unusual; for large positive values of H_0, the cells are wrinkled, and increasing p reduces the number of wrinkles. Such shapes could be induced by modifications of the skeleton or changes in the composition of the bilayer. It would be interesting to systematically compare the shapes obtained in such simulations of an elastic membrane with the predictions made for fluid membranes [which neglect, however, thermal fluctuations and assume a rotational symmetry (2–6)]. Although for the elastic parameters used in the simulation described in Fig. 1 a fluid membrane should also form a discocyte (4), this does not need to be always true. Indeed, for large values of H_0, fluid membranes are expected to be formed of several connected spheres (6), whereas in our simulations we observe the mentioned wrinkled shapes. This is a direct consequence of the fixed connectivity of the network.

Another phenomenon exhibited in our simulations is the "unbinding" of adhering cells, similar to the unbinding transition predicted (24) and then observed (25) in a stack of fluid bilayer membranes. Fig. 2 shows the interaction of two identical "discocytes" through a short-ranged attractive potential, h. In our simulation we have used a simple square-well attraction of range $l = 1.4$ and the depth h. For intermediate values of h (Fig. 2*B*), the cells are bound together and their form is very close to the free shape [as, e.g., in a "rouleau" formation of erythrocytes (26)]. By increasing h one can induce shape transformation; the cells in Fig. 2*A* are cup-like since the interaction energy is higher. When h is lowered below some critical value, entropic repulsion overcomes the attractive potential and the cells "unbind" (Fig. 2*D*). One can also induce unbinding by increasing the temperature or decreasing the bending rigidity (13, 24).

A detailed scaling analysis of the phenomena described above, analogous to those done for simulations of hypothetical two-dimensional vesicles (16) or planar membranes (27), lies beyond the scope of this paper. Such studies make possible quantitative analysis of experiments on erythrocytes and vesicles, especially if one extends the present work to fluid membranes and realistic skeleton–membrane structures. Experimentally, it should be possible to verify our predictions on unbinding and adhesion by using electrostatic forces or adhesive molecules. In addition, our study shows that computer simulations could help in the near future in understanding some of the simplest collective physical phenomena taking place in cellular systems.

We thank M. Bessis and E. Sackmann for discussions. A.C.M. is at a laboratoire associé au Centre National de la Recherche Scientifique.

1. Elgsaeter, A., Stokke, B. T., Mikkelsen, A. & Branton, D. (1986) *Science* **234,** 1217–1223.
2. Canham, P. B. (1970) *J. Theor. Biol.* **26,** 61–81.
3. Bull, B. S. & Brailsford, D. (1989) in *Red Blood Cell Membranes*, eds. Agre, P. & Parker, J. C. (Dekker, New York), pp. 401–421.
4. Deuling, H. J. & Helfrich, W. (1976) *Biophys. J.* **16,** 861–868.
5. Peterson, M. A. (1985) *Mol. Cryst. Liq. Cryst.* **127,** 159–186.
6. Svetina, S. & Zeks, B. (1989) *Eur. Biophys. J.* **17,** 101–111.
7. Gratzer, W. B. (1981) *Biochem. J.* **198,** 1–8.
8. Evans, E. A. (1983) *Biophys. J.* **43,** 27–30.
9. Fricke, K., Wirthensohn, K., Laxhuber, R. & Sackmann, E. (1986) *Eur. Biophys. J.* **14,** 67–81.
10. Schneider, M. B., Jenkins, J. T. & Webb, W. W. (1984) *J. Phys. (Paris)* **45,** 1457–1472.
11. Engelhardt, H., Duwe, H. P. & Sackmann, E. (1985) *J. Phys. (Paris)* **46,** L395–L400.
12. Bivas, I., Hanusse, P., Botherel, P., Lalanne, J. & Agnerre-Chariol, O. (1987) *J. Phys.* **48,** 855–867.
13. Nelson, D., Piran, T. & Weinberg, S., eds. (1989) in *Statistical Mechanics of Membranes and Surfaces* (World Sci., Singapore).
14. Helfrich, W. (1973) *Z. Naturforsch.* **28c,** 693–703.
15. Brochard, F. & Lennon, J.-F. (1975) *J. Phys. (Paris)* **36,** 1035–1047.
16. Leibler, S., Singh, R. P. R. & Fisher, M. E. (1987) *Phys. Rev. Lett.* **59,** 1989–1992.
17. Ostrowsky, N. & Peyraud, J. (1981) *J. Chem. Phys.* **77,** 2081–2087.
18. Aronovitz, J. A. & Lubensky, T. C. (1988) *Phys. Rev. Lett.* **60,** 2634–2637.
19. Guitter, E., David, F., Leibler, S. & Peliti, L. (1988) *Phys. Rev. Lett.* **61,** 2949–2952.
20. Zilker, A., Engelhardt, H. & Sackmann, E. (1987) *J. Phys. (Paris)* **48,** 2139–2151.
21. Kantor, Y., Kardar, M. & Nelson, D. R. (1986) *Phys. Rev. Lett.* **57,** 791–794.
22. Liu, S.-C., Derick, L. H. & Palek, J. (1987) *J. Cell Biol.* **104,** 527–536.
23. Binder, K. & Heermann, D. W. (1989) *Monte-Carlo Simulations in Statistical Physics* (Springer, Berlin).
24. Lipowsky, R. & Leibler, S. (1986) *Phys. Rev. Lett.* **56,** 2541–2544.
25. Mutz, M. & Helfrich, W. (1989) *Phys. Rev. Lett.* **62,** 2881–2884.
26. Fritz, O. G. (1984) *Biophys. J.* **46,** 219–225.
27. Leibler, S. & Maggs, A. C. (1989) *Phys. Rev. Lett.* **63,** 406–409.